Trypanosoma cruzi senses intracellular heme levels and regulates heme homeostasis by modulating *Tc*HTE protein expression

Lucas Pagura*†[1], Evelyn Tevere*, Marcelo L. Merli*[2], Julia A. Cricco*†[3]

From the *Instituto de Biología Molecular y Celular de Rosario (IBR), Consejo Nacional de Investigaciones Científicas y Técnicas CONICET – Facultad de Ciencias Bioquímicas y Farmacéuticas, Universidad Nacional de Rosario UNR. Suipacha 531, S2002LRK, Rosario, Argentina.
†Área Biofísica, Departamento de Química Biológica, Facultad de Ciencias Bioquímicas y Farmacéuticas, Universidad Nacional de Rosario UNR. Suipacha 531, S2002LRK, Rosario, Argentina.

Running Tittle: *Trypanosoma cruzi* regulates heme transport *via Tc*HTE

[1]Present address: Department of Immunology and Infectious Diseases, Harvard T.H. Chan School of Public Health, 655 Huntington Avenue, FXB 217, Boston, MA 02115, USA.
[2]Present address: Department of Microbiology and Cell Science, Genetics Institute, Institute of Food and Agricultural Sciences, University of Florida, 2033 Mowry Road, PO Box 103610, Gainesville, FL 32610-3610, USA.

[3]to whom correspondense should be address: Julia A. Cricco, Instituto de Biología Molecular y Celular de Rosario (IBR), Consejo Nacional de Investigaciones Científicas y Técnicas CONICET – Facultad de Ciencias Bioquímicas y Farmacéuticas, Universidad Nacional de Rosario UNR. Suipacha 531, S2002LRK, Rosario, Argentina. Tel.: +54-341-4350661 ext 133; E-mail: cricco@ibr-conicet.gov.ar

Keywords: *Trypanosoma cruzi*, Chagas disease, heme, heme transport, heme responsive gene, parasites.

ABSTRACT

Heme is an essential cofactor for many biological processes in aerobic organisms. Most of them can synthesize it *de novo* via a conserved pathway. *Trypanosoma cruzi*, the etiological agent of Chagas disease, as other trypanosomatids relevant for human health, are heme auxotrophs; thereby they must import it from the hosts. *Tc*HTE protein is involved in *T. cruzi* heme transport, although its specific role remains elusive. In the present work we study endogenous and recombinant *Tc*HTE in the different life cycle stages of the parasite, in order to approach to its function in heme transport and heme homeostasis. We have confirmed that *Tc*HTE belongs to the HRG protein family, it is predominantly detected in replicative stages (epimastigote and amastigote) and localized mainly in the flagellar pocket of the parasite. We have also demonstrated that *T. cruzi* epimastigotes can sense intracellular heme content by an unknown mechanism and are able to modulate the expression of *Tc*HTE in order to regulate heme transport. Based on these results, we propose a model in which *T. cruzi* regulates heme transport activity adjusting the amount of *Tc*HTE present in the cell. This work is, to our knowledge, the first study of an endogenous trypanosomatid HRG protein. The elucidation and characterization of heme transport and homeostasis will contribute to a better understanding of the biology of *T. cruzi*, a parasite relevant for human health.

Heme is an iron-containing protoporphyrin involved in many biological processes related with oxygen and other diatomic gases transport and sensing, oxidative metabolism, stress response, gene transcription, microRNA processing, among others (1–4). This molecule is essential for all the aerobic organisms, and most of them are able to synthesize it *via* a conserved pathway (5–7). Exceptions to this are the trypanosomatids. Although they present many heme-proteins involved in essential metabolic pathways, trypanosomatids are aerobe organisms lacking any complete heme synthesis pathway (8), so they must

scavenge this molecule from the environment or host (9). In this group are included trypanosomatids relevant for human health as *Trypanosoma cruzi* (Chagas disease), *Trypanosoma brucei* (sleeping sickness) and *Leishmania spp*. (visceral, cutaneous and muco-cutaneous leishmaniasis). *T. cruzi* undergoes a complex life cycle alternating between two hosts and displaying at least four developmental stages that are morphologically and metabolically different. Epimastigotes are the proliferative form that lives in the gut of the insect vector. This form differentiates into metacyclic trypomastigotes, the infective form that once in the mammal is able to infect any nucleated cells and differentiate into amastigotes, the intracellular proliferative form. After some replication cycles, amastigotes differentiate into bloodstream trypomastigotes that are released from the cells into the bloodstream, spreading the infection throughout the organism. When the insect vector feeds from an infected mammal, the bloodstream trypomastigotes differentiate into epimastigotes and become able to replicate in the gut of the insect (10).

In the last years, proteins presenting homology sequence to *Ce*HRG-4 (*Caenorhabditis elegans* Heme Responsive Gene 4) (11) have been described in trypanosomatids. LHR1 (*Leishmania* Heme Response-1, from *Leishmania amazonensis*) was the first postulated as a heme transporter. LHR1 mRNA responds to heme availability in the environment, confirming it as a member of the HRG family (12). Also, heme uptake mediated by LHR1 results relevant for the virulence of *L. amazonensis* (13, 14). We described a homologous protein in *T. cruzi*, named *Tc*HTE (*T. cruzi* Heme Transport Enhancer), that plays a critical role in heme transport and is found mainly in the flagellar pocket of *T. cruzi* (15). More recently, *Tb*HRG (*T. brucei* Heme Responsive Gene) was described in *T. brucei* and postulated to be involved in heme transport as free-heme or in the salvage of heme from hemoglobin degradation (16, 17). LHR1, *Tc*HTE and *Tb*HRG present similar growth performance when expressed in *Saccharomyces cerevisiae hem1*Δ, allowing this knock out cells to growth in a medium supplemented with low heme. Also, the over-expression of recombinant versions of these trypanosomatid genes in the corresponding native organisms causes an increment in the intracellular heme concentration, confirming their role in heme transport (12, 15, 16). Bioinformatic studies have shown that these trypanosomatid proteins present significant similarities to the predicted topology of *Ce*HRG-4 (11), such as 4 trans-membrane domains (12, 15, 16). However, it remains unclear how the HRG proteins work and which is their precise role in heme transport. They could form the specific heme transporters, in this case, they must assemble into a homo-trimer or homo-tetramer to form a channel or a pore. Or, they could be an essential component of a heteromeric complex responsible for heme transport activity. Moreover, considering that the gene expression in trypanosomatids is not regulated by canonical transcription factors (18, 19), it is not clear how the expression of HRG genes is regulated by heme.

In this work, we present the study of the endogenous *Tc*HTE. Our data clearly demonstrate that *Tc*HTE directly responds to heme (as both mRNA and protein) similar to LHR1 (12), confirming *Tc*HTE as a member of HRG family. Using different heme fluorescent analogs, we proved that epimastigotes sense intracellular heme concentration and consequently modulate the amount of *Tc*HTE to diminish or increase heme uptake. Besides, the expression of recombinant *Tc*HTE enhances replication of intracellular amastigotes, probably increasing heme uptake from the cytoplasm of the infected cell where its availability could be a limiting growth factor. Interestingly, this finding suggests that heme induces the intracellular replication of amastigotes.

Remarkably, our results have shown that heme transport activity in *T. cruzi* is tightly modulated by the presence or absence of *Tc*HTE.

Results

The accumulation of *Tc*HTE (mRNA and protein) changes through the different life-cycle stages of *Trypanosoma cruzi*

*Tc*HTE was previously described as a critical protein for heme transport in *T. cruzi*, presumably being part of the heme transporter and/or regulating this activity (15). To expand our knowledge on *Tc*HTE, we first obtained specific polyclonal antibodies against *Tc*HTE (Supporting information S1) that were used to detect and analyze the endogenous protein along the *T. cruzi* life-cycle stages. The Western blot assays revealed that intensity of *Tc*HTE signal was higher in samples taken from amastigotes and epimastigotes (replicative stages) and it was almost undetectable

for trypomastigotes (the infective and non-replicative stage), as it is shown in Figure 1A. Surprisingly, the intensity of the band obtained from epimastigotes varied together with hemin concentration in the culture medium, being more intense at the lower hemin concentrations (see below). In this case, epimastigotes were incubated 3 days in LIT-10% FBS with 0, 5 and 20 µM hemin, without previous heme starvation. Also, we analyzed the accumulation level of *Tc*HTE mRNA by qRT-PCR assay. The amount of *Tc*HTE mRNA (normalized to epimastigotes cultured with 5 µM hemin) was significantly higher in samples taken from epimastigotes than amastigotes, and both (epimastigotes and amastigotes) were significantly higher compared to trypomastigotes, as it is shown in Figure 1B. These results indicate that *Tc*HTE was upregulated at mRNA and protein level in the replicative stages compared to the infective stage.

Variation in the concentration of hemin affects the amount of *Tc*HTE detected in replicative life-cycle stages

To explore if changes in the amount of hemin added to the culture medium could modulate the amount of *Tc*HTE present in cells, first we revisited the growth conditions reported for epimastigotes. Previously we have shown that *T. cruzi* incorporates heme and heme analogues (HAs) in the replicative life-cycle stages to fulfill the requirements for this cofactor. The addition of 5-20 µM hemin to the medium did not affect epimastigote growth and, in stationary state, the intracellular heme concentration was approximately the same in both cases. However, higher concentration of hemin produced a growth defect, being highly toxic at 100 µM (15). Furthermore, we analyzed the effect caused by an increment in hemin concentration in the medium but below lethal concentrations (50 µM or less). Epimastigotes routinely maintained in a medium with 5 µM hemin were collected, washed and starved for heme for 72 h (medium without hemin). After that, parasites were cultured with 0, 5, 20 or 50 µM hemin for seven days. Then, cultures were diluted in fresh media (maintaining the same hemin concentration) and the growth was followed for other seven days (Figure 2A). At the end of the first week slight differences in the total parasite number were observed in epimastigotes growing at 0, 5 and 20 µM hemin and a moderated negative effect at 50 µM hemin. However, during the second week, the negative effect produced by low (no hemin added) and higher hemin concentrations (20 and 50 µM) was more severe. The addition of 5 µM hemin resulted the optimal concentration to allow parasite's growth in this condition. Also, on the third and seventh days of the first week, samples were collected, stained with Giemsa reagent and analyzed by optical microscopy (Figure 2B). The epimastigotes challenged to growth with 0 or 5 µM hemin presented a conserved elongated shape, as typically described for epimastigotes. However, those maintained with 20 or 50 µM hemin presented a rounded shape, possibly a consequence of a potential toxic effect caused by the amount of hemin present in these media. The accumulation of *Tc*HTE protein in epimastigotes was analyzed by Western blot assays after 72 h of incubation in the different conditions. The protein signal was observed in samples taken from 0 and 5 µM hemin, but almost undetectable at 20 or 50 µM hemin, as it is shown in Figure 2C (left panel), in agreement with results reported in Figure 1A.

The accumulation of *Tc*HTE in intracellular amastigotes was also evaluated in samples treated with or without the addition of hemin. In this case, infected monolayered Vero cells routinely maintained in DMEM-2% FBS, were incubated without (as control) or with 20 µM hemin for 24 h. Then, amastigotes were purified and the presence of *Tc*HTE was analyzed by Western blot. These results are presented in the right panel of Figure 2C, the signal corresponding to *Tc*HTE was clearly detected in samples from control amastigotes (incubated without hemin), but the addition of 20 µM hemin caused a reduction in the amount of *Tc*HTE, being the protein signal almost undetectable.

In summary, *Tc*HTE was detected in the replicative forms of *T. cruzi,* but more importantly, it was more abundant in epimastigotes and amastigotes maintained (or treated) under heme deprivation or low heme availability.

The amount of *Tc*HTE (mRNA and protein) detected in epimastigotes responds to changes in the concentration of hemin.

To proceed our studies on *Tc*HTE, we evaluated how it responds to changes in hemin concentration in the medium (as protein and mRNA). Figure 1A and 2C have shown that the

intensity of the *Tc*HTE signal increases with a diminution of hemin concentration in the medium. Then, we analyzed if the accumulation of *Tc*HTE mRNA is affected when epimastigotes were challenged to lower or higher concentration of hemin. Briefly, epimastigotes maintained with 0 or 20 µM hemin for 3 days were collected, washed and incubated with 0, 5 and 20 µM hemin for 18 h. In both cases, the changes in the amount of *Tc*HTE mRNA relative to GAPDH (housekeeping gene) were quantified by qRT-PCR and results are presented in Figure 3A. When epimastigotes maintained with 20 µM hemin were changed to a medium without the addition of hemin (0 µM) the amount of *Tc*HTE mRNA significantly increased (at least 3 times) (Figure 3A right panel). On the other hand, when epimastigotes maintained without hemin were changed to 5 or 20 µM hemin, the amount of accumulated *Tc*HTE mRNA significantly decreased in both cases (approximately 2 and 3 times, respectively) (Figure 3A, left panel).

Additionally, the amount of *Tc*HTE protein was evaluated by Western blot assays. Briefly, epimastigotes routinely maintained with 5 µM hemin were transferred to 30 µM hemin for eight days (Figure 3B). Samples were taken every hour along the first day (from 10 to 18 h, Figure 3B bottom panel) and after that, once per day for seven days. On the eighth day, epimastigotes were washed, transferred to fresh medium without the addition of hemin (0 µM), cultured for up to day fourteen, and samples were taken periodically (Figure 3B). All samples were processed and subject to Western blot assay to test the accumulation of *Tc*HTE. As sample processing and loading control, the same membranes were blotted against α-tubulin. The results, presented in Figure 3B (upper panel), show that signal of *Tc*HTE protein almost disappeared 24 h after epimastigotes were moved from 5 to 30 µM hemin. The inset of Figure 3B (bottom panel) clearly shows that *Tc*HTE signal became almost undetectable after 15-17 h. On the other hand, when epimastigotes were transferred from 30 µM hemin to a hemin-free medium, 48 h were required to restore *Tc*HTE signal. In addition, we quantified the intracellular heme content in epimastigotes (which were previously starved for heme for 48 h) after 18 and 24 h of incubation with 0, 5, 30 and 50 µM hemin. There was a slight -but not significant- difference in the intracellular heme concentration in samples taken at 18 h of incubation at 5, 30 and 50 µM hemin. These differences decreased and the intracellular heme concentration progressed to almost the same value after 24 h of incubation, approximately 3 nmol/10^9 parasites as (Figure 3C). The intracellular heme quota could be estimated and for epimastigotes Dm28c it was approximately $3x10^{-9}$ nmoles of heme/parasite

These results confirmed *Tc*HTE as a member of HRG family since mRNA accumulation and protein level were regulated by heme in *T. cruzi* (Supplementary Information S2, phylogenetic tree). However, there is no evidence if any intracellular or extracellular signal trigger changes in *Tc*HTE accumulation.

Epimastigotes can sense intracellular heme (and HAs) to modulate *Tc*HTE protein level.

Fluorescent heme analogs (HAs) have been used to evaluate heme transport activity in *T. cruzi* (15, 20, 21). Also, we have shown that *T. cruzi* can selectively transport heme (or HAs) only in the replicative stages (15). Based on this capability, we designed a strategy to evaluate if epimastigotes can sense intracellular or environmental heme (or HAs) to modulate *Tc*HTE expression. First, epimastigotes were challenged to grow under non-toxic concentration of "total hemes" of 20 µM or less ("total hemes" is referred to hemin plus different HAs, or total metallated-porphyrins), and *Tc*HTE protein was evaluated by Western blot assay. The growth profile of epimastigotes in a medium containing hemin (20 µM or 5µM) or 5 µM hemin + 15 µM HAs (20 µM of total hemes) is shown in Figure 4A. Surprisingly, epimastigotes incubated with 5 or 20 µM hemin or with 5 µM hemin plus 15 µM SnMP (Sn(IV) mesoporphyrin IX) did not show any significant difference in the growth's profile. On the other hand, those incubated with 5 µM hemin plus 15 µM ZnMP (Zn(II) mesoporphyrin IX), were severely affected. Samples were taken at the third day of the curve and the presence of HAs inside cells was analyzed by confocal microscopy and direct fluorescent measurement in a similar way as we previously reported for heme/HAS transport activity (15). Figure 4B and C show that epimastigotes incubated with SnMP (5 µM hemin plus 15 µM SnMP) did not exhibit any significant fluorescent signal detected by direct measurements of fluorescence or

confocal microscopy, suggesting that it was not imported, or it was rapidly exported. In any of these cases, SnMP did not remain inside the cell. On the other hand, epimastigotes incubated with ZnMP (5 µM hemin plus 15 µM ZnMP), have shown an intense fluorescence signal, detected by confocal microscopy and direct fluorescence measurements, corresponding to its incorporation by the cell. These observations are in agreement with our previous results in which we have shown that ZnMP was internalized by *T. cruzi*, but SnMP was not incorporated (15). Also, the absence of SnMP fluorescent signal inside the cell could explain why the treatment with this HA did not affect the growth of epimastigotes. The effect of these HAs on *Tc*HTE accumulation was analyzed by Western blot assay in samples taken after three days of incubation with the HAs (0, 5, 20 µM hemin, 5 µM HAs or 5 µM hemin + 15 µM HA), and the results are shown in Figure 4D. Interestingly, the signal corresponding to *Tc*HTE was observed in samples taken from epimastigotes incubated with 0 or 5 µM hemin, 5 µM of SnMP, 5 µM of hemin plus 15 µM of SnMP (20 µM total hemes), and with 5 µM of ZnMP. On the other hand, *Tc*HTE was not detected in samples taken from epimastigotes incubated with 5 µM of hemin plus 15 µM of ZnMP or with 20 µM of hemin. These results indicate that 15 µM of SnMP (plus 5 µM of hemin) which is not maintained inside the parasite, did not affect *Tc*HTE accumulation. On the other hand, 15 µM of ZnMP (plus 5 µM of hemin), which is accumulated inside cell, provoked a reduction on *Tc*HTE protein level similarly to the reduction produced by the incubation with 20 µM of hemin.

When we analyzed intracellular heme content, as it is shown in Figure 4E, we observed that the treatment with both HAs (ZnMP and SnMP) significantly reduced intracellular heme content, indicating that somehow SnMP blocked heme uptake causing a drop in the intracellular heme concentration. It is interesting to mention that only hemin and the HA that was internalized (ZnMP) were able to reduce *Tc*HTE accumulation. On the other hand, SnMP -which does not remain inside the cell- did not affect *Tc*HTE expression.

r*Tc*HTE is localized in the flagellar pocket region of *T. cruzi*

Previously, we determined that recombinant *Tc*HTE.His-GFP (*rTc*HTE.His-GFP) is localized in the flagellar pocket region of epimastigotes (15). Here we also analyzed the localization of r*Tc*HTE.His-GFP in trypomastigotes and intracellular amastigotes. Briefly, recombinant epimastigotes (15) were submitted under metacyclogenesis process to produce recombinant trypomastigotes that were later used to infect monolayered Vero cell line. Three days post infection, infected cells containing recombinant amastigotes were analyzed by confocal microscopy to visualize the green signal of the *rTc*HTE.His-GFP in amastigotes. Also, seven days post infection, trypomastigotes containing *rTc*HTE.His-GFP were collected and processed for confocal microscopy analysis (Figure 5A). The signal corresponding to r*Tc*HTE.His-GFP was punctually localized in a region between the nucleus and kinetoplast (blue signal, DAPI staining) that could overlap with the flagellar pocket region in trypomastigotes as it was previously shown for epimastigotes (15). The images recorded for intracellular amastigotes showed that r*Tc*HTE.His-GFP signal is highly intense and punctuated in a precise region over the plasma membrane that could overlap with the flagellar pocket region. However, several amastigotes have shown a fluorescent signal distributed along the plasma membrane. This difference observed in the localization of r*Tc*HTE.His-GFP in amastigotes could be an effect of the protein over-expression (r*Tc*HTE.His-GFP) or indicate that *Tc*HTE changes localization in the intracellular life-cycle stage.

r*Tc*HTE.His-GFP enhances replication of amastigotes.

The replication of intracellular amastigotes was analyzed in wild type and recombinant parasites over-expressing r*Tc*HTE.His-GFP. Briefly, monolayers of Vero cells were infected with wild type or recombinant trypomastigotes over-expressing r*Tc*HTE.His-GFP. At 48 h post infection, infected cells were fixed and stained with Giemsa and amastigotes counted (Figure 5B). Cells infected with recombinant trypomastigotes over-expressing r*Tc*HTE.His-GFP have contained significantly more intracellular amastigotes than those infected with wild type parasites (29.74 ± 2.33 and 18.43 ± 1.35 amastigotes/infected-cell, respectively, $p<0.0001$). This result suggests that the over-expression of *Tc*HTE increased amastigote

replication rate in a low free-heme environment as the cellular cytosol.

Discussion

Heme is an essential cofactor for aerobic organisms. Most of them are able to synthesize heme throw a conservative pathway. Also, it is well established that free-heme is not found in any living cell due to the toxicity exhibited by this compound and every cell, must have strict control in heme homeostasis to avoid its harmful effect. *T. cruzi*, as well as other trypanosomatids, does not synthesize it and for this reason, these parasites needs to take the cofactor from its host to fulfill the heme quota (9, 22). Once heme is inside the cell, transporters, chaperons and/or carriers must be involved in heme transport and trafficking. During the last years, several proteins involved in heme transport have been described in trypanosomatids, such as LHR1 in *Leishmania spp.* (12–14), *Tb*HRG in *Trypanosoma brucei* (16, 17), and *Tc*HTE in *Trypanosoma cruzi* (15). And most recently a protein identified in *L. major*, named *Lm*FLVCRb and member of a Major Facilitator Superfamily, was described as a heme importer in this organism (23). The latest might be involved in free-heme transport in *L. major* and probably overlapping some functions with *Lm*HR1. However, the mechanism of heme transport and the undoubtedly identity of the transporters and their regulation have not been completely unraveled nor in *T. cruzi* neither in other trypanosomatids.

In this work we present data that clarify the relationship between *Tc*HTE (as mRNA and endogenous protein) and heme transport activity in *T. cruzi*. The analysis of mRNA accumulation by quantitative RT-PCR has indicated that the amount of *Tc*HTE mRNA was significatively higher in the replicative life-cycle stages of *T. cruzi*, compared to the infective one. The attainment of antibodies against *Tc*HTE allowed us to present, to our knowledge, the first study on an endogenous trypanosomatid's proteins with homology to HRG ones. In this case, *Tc*HTE was clearly detected in the replicative stages (epimastigotes and amastigotes), and almost undetectable in trypomastigotes. Precisely, our data shows that *Tc*HTE mRNA and protein were more abundant in stages where *T. cruzi* is able to import heme (or heme analogs HAs) (15). In addition, changes in the amount hemin added to the medium affected the amount of *Tc*HTE mRNA detected in epimastigotes, being higher at low concentration or absence of hemin and lower at higher concentration of this cofactor. This observation corroborates that *Tc*HTE mRNA respond to heme as well as LHR1 (12), confirming *Tc*HTE as a member of the Heme Response Gene (HRG) family (11). It is important to note that *Leishmania* (12) and *T. cruzi* HRGs respond to heme but not *Tb*HRG (17), suggesting that those gene products might be under different regulations and/or play different roles in heme transport.

Interestingly, the profile of *Tc*HTE protein accumulation in epimastigotes and amastigotes suggests a dependence on the amount of heme available in the environment (medium/host cytosol). Our data obtained from epimastigotes shifted from a rich to poor (and poor to rich) heme containing medium suggest that heme starvation caused a drop in intracellular heme concentration below the optimal, then the expression of *Tc*HTE augmented allowing the detection of this protein by Western blot. Once the internal heme quota was satisfied, the heme transport should reach a stationary state and, consequently, *Tc*HTE protein level decreased (almost undetectable by Western blot). These results strongly suggest that heme requirement could modulate *Tc*HTE protein level (and mRNA) in the parasite, being *Tc*HTE more abundant when *T. cruzi* needs to incorporate heme. Also, the amount of intracellular heme quantified in epimastigotes challenged to different amounts of hemin, demonstrates that *T. cruzi* incorporates the amount of heme that needs, despite the amount of heme available in the medium. In other words, epimastigotes incorporate as much heme as it is necessary to supply its "heme quota". We cannot exclude heme degradation as part of a mechanism to control intracellular heme, but genes encoding for enzymes with homology sequence to heme oxygenase has not been identified in the genome of *T. cruzi* (24). Presumably, heme degradation *via* heme oxygenase like activity previously reported (24) would not be enough to get rid of any excess of heme when epimastigotes are exposed at high concentration of hemin. Under this premise, the amount of intracellular heme could be mainly controlled by its transport and the fact that *Tc*HTE increases (mRNA and protein) when *T. cruzi* needs to incorporate heme and decreases when heme

quota is satisfied is consistent with this protein being the heme transporter or an essential part of it.

To clarify if *Tc*HTE responds to signal of extracellular or intracellular heme, we took advantage that *T. cruzi* can selectively import HAs (ZnMP, but not SnMP) (15). In this work we challenged epimastigotes to grow in presence of hemin (5 μM) competing with ZnMP or SnMP (15 μM of HA). The concentration of intracellular heme was significantly lower in those samples incubated with hemin plus HA, indicating that these compounds compete and/or interfere with heme uptake. Additionally, ZnMP was accumulated inside the parasite but not SnMP, as it was revealed by confocal microscopy and direct fluorescence measurements. Interestingly, even though intracellular heme was significatively lower in samples treated with ZnMP, *Tc*HTE was almost undetectable by Western blot. On the other hand, epimastigotes treated with SnMP (and hemin) which also presented lower intracellular heme, showed a strong signal corresponding to *Tc*HTE, similar to the signal obtained from those parasites incubated with low hemin in the medium. These results indicate that epimastigotes internalized ZnMP and hemin indistinctly, contributing to the concentration of "total hemes" (heme + ZnMP) and both are sensed by the parasite. On the other hand, given that SnMP was not detected inside the cell, it is not sensed as "heme" by the parasite, then, it is reasonable to conclude that SnMP would not affect *Tc*HTE expression. The fact that SnMP is not internalized or maintained inside cell, is also consistent with the no effect observed in the parasite growth profile. These results strongly suggest that epimastigotes can sense intracellular heme, independently of the amount of hemin present in the medium and modulate *Tc*HTE expression according to the necessity to increase/decrease the incorporation of heme. It is not known which signal is sensed, heme itself, a heme-chaperone concentration or a modification in any "sensor", that indicates that the parasite has taken enough heme to supply its quota. However, these evidences place *Tc*HTE playing an essential role in heme homeostasis in *T. cruzi*.

Other point explored in this work was the localization of the *Tc*HTE protein in other life-cycle stages beside the epimastigote one, where r*Tc*HTE.His-GFP was localized in the flagellar pocket region of epimastigotes (15). Although endogenous *Tc*HTE was almost undetectable in trypomastigotes, the expression of the r*Tc*HTE.His-GFP has allowed its detection and localization in the flagellar pocket region, maintaining the same location as in epimastigotes. Also, r*Tc*HTE.His-GFP was evaluated in intracellular amastigotes. All the analyzed images have shown an intense fluorescent signal punctually localized in the region of the flagellar pocket, but some of them also displayed a light signal on the plasma membrane. We could not discern if the fluorescent signal detected around the plasma membrane was due to a mislocation caused by the over-expression of the recombinant protein or because the protein location changed in amastigote stage. It is important to mention that amastigotes can express other proteins in its surface and it is postulated that they could interact with host cell mitochondria via the flagellum (25). In this scenario, the interaction between flagellum and mitochondrial host could increase the proximity of the flagellar pocket to this organelle improving nutrient acquisition, as for heme. Summarizing these results, it is reasonable to postulate that *Tc*HTE is localized in the flagellar pocket region where it facilitates heme transport in *T. cruzi*. Interestingly, we did not detect r*Tc*HTE.His-GFP in internal vesicles as it was reported by the recombinant versions of *Leishmania* HRG protein (LaHR1 or LmHR1)(12, 16) and *T. brucei*, *Tb*HRG (16) or in the flagellar membrane of procyclic stage of *T. brucei* (17).

We also evaluated if the replication of intracellular amastigotes could be affected by heme. However, it was challenging to increase intracellular heme concentration of the host cells without injured them. Since the presence of recombinant *Tc*HTE increased heme uptake of epimastigotes (15), we used r*Tc*HTE.His-GFP over-expressing amastigotes for this study because the addition of significant amounts of hemin before or during the infection, or the incubation of infected cells with high levels of hemin for the time required for this experiment resulted toxic for the host cells. Surprisingly, a significantly higher number of intracellular amastigotes was determined in cell lines infected with the recombinant parasites compared with those infected WT ones, confirming that *Tc*HTE could modulate heme transport and heme modulates cellular replication as it was proposed for *L. amazonensis* and LHR1 where the deletion of one copy of genomic LHR1 impaired

intracellular replication of amastigotes of this *L. amazonensis* (14). In summary, it is reasonable to postulate that the ability of intracellular amastigotes to incorporate more heme enhances its replication rate.

Based on the results presented here, we propose a model for *Tc*HTE and its role in heme transport in *T. cruzi* that is represented in Figure 6. In epimastigotes, under stationary state of heme flux, the protein level of *Tc*HTE is low, almost undetectable by Western blot. The parasite maintains constant the intracellular heme concentration, presumably maintaining low the heme import activity. Under heme deprivation (heme starvation) epimastigotes sense low intracellular heme, the expression of *Tc*HTE gene increases, more protein is assembled in the flagellar pocket region as heme transporter or part of it, and heme transport activity raises. Once the intracellular heme concentration is satisfied/fulfilled, a signal (still unknown) triggers the mRNA and also the extra-protein degradation and the heme transport activity decreases to stationary level. Based on its size and its predicted structural features, *Tc*HTE might be the heme transporter, as a homo-trimer or homo-tetramer protein. Also, *Tc*HTE could be part of the heme transporter, forming a hetero-complex. Nevertheless, we cannot exclude *Tc*HTE acting only as a regulatory subunit of the heme transporter. In this scenario, when heme transport activity is required, *Tc*HTE is synthesized and assembled to build or activate the transporter. The constant detection of endogenous *Tc*HTE in intracellular amastigotes, is consistent with the fact that available heme in the cytoplasm of host cells is very low (labile-heme was estimated in different eukaryotic cells, in yeast 20 - 40 nM (26), Heck293 cells approximately 450 nM, (27), IMR90 lung fibroblast cells, approximately 614 nM (28)) and its presence is necessary to guarantee enough heme uptake in this life-cycle stage. The reduction of this protein signal when extra hemin was added to the infected cells, confirms our model for *Tc*HTE.

In summary, *Tc*HTE responds to intracellular heme, as mRNA and protein, then we can confirm it as a member of HRG family protein and based on this finding it might be renamed as *Tc*HRG. *T. cruzi* epimastigotes can manage intracellular heme concentration by controlling its transport in replicative life-cycle stages where the presence of *Tc*HTE/*Tc*HRG is essential to this process. *T. cruzi* can sense intracellular heme, by any still unknown mechanism, and adjust *Tc*HTE expression and accumulation in order to promote or reduce heme transport activity. Evidences presented here strongly suggest that *Tc*HTE/*Tc*HRG is a relevant part of the heme transporter, and its localization in the flagellar pocket region in all life-cycle stages evaluated indicates that it is probably involved only in free-heme transport, although we cannot exclude its participation in the salvage of heme from Hb degradation. In this scenario, the characterization of heme transport and distribution will contribute to the better understanding of the biology and biochemistry of *T. cruzi,* the etiological agent of the most prevalent parasitic disease in several countries of America (https://www.who.int/news-room/fact-sheets/detail/chagas-disease-(american-trypanosomiasis). This, in turn, will enable the identification of novel proteins playing essential roles which might act as possible targets for new drug development against Chagas disease.

Experimental procedures

Reagents. Dulbecco's Modified Eagle Medium (DMEM) was obtained from Life Technologies, Fetal Bovine Serum (FBS) from Internegocios SA. FBS was heat-inactivated at 56°C for an hour. Hemin, ZnMP (Zn(II) mesoporphyrin IX) and SnMP (Sn(IV) mesoporphyrin IX) were obtained from Frontier Scientific. Hemin stock solution was prepared 1 mM in 50% (v/v) EtOH:0.01 M NaOH, sterilized by filtration using a 22 µm syringe disposable filter, fractionated, and stored at -80 °C. Heme concentration in the stock solution was confirmed by spectroscopic measurements at 385 nm, ε^{385}= 58400 $M^{-1}cm^{-1}$ (26). ZnMP and SnMP were dissolved in DMSO at a final concentration of 20 mM and stored at -80 °C. The heme analogues (HAs) working solutions were prepared dissolving the stock solution in 0.01 M NaOH at a final concentration of 1 mM.

Parasites and cell lines. All experiments were performed using *T. cruzi* Dm28c strain and all the infections were carried out in Vero cell line (ATCC CCL-81, already available in our laboratory). Epimastigotes (WT and recombinant over-expressing *Tc*HTE.HIS-GFP) of *T. cruzi* were maintained in mid-log phase by periodic dilutions

in Liver Infusion Tryptose (LIT) medium supplemented with 10% heat inactivated FBS (LIT-10% FBS) and 5 µM hemin (15), at 28 °C. The Vero cell line was routinely maintained in DMEM medium supplemented with 0.15% (w/v) $NaHCO_3$, and 10% heat inactivated FBS (DMEM-10% FBS) at 37 °C in a humid atmosphere containing 5% CO_2. During the *T. cruzi* infections, Vero cells were incubated in DMEM medium supplemented 2% heat inactivated FBS (DMEM-2% FBS) at 37 °C in a humid atmosphere containing 5% CO_2. Metacyclic trypomastigotes (WT and recombinant over-expressing *Tc*HTE.HIS-GFP) were obtained by spontaneous differentiation of epimastigotes at 28 °C after two weeks of culture without dilution. Metacyclic trypomastigotes were used to infect monolayered Vero cells and to obtain cell-derived trypomastigotes after 5-6 days post-infection. Intracellular amastigotes were obtained 2- or 3-days post infection of monolayered Vero cell line with cell-derived trypomastigotes. The homogeneity of the obtained *T. cruzi* forms was evaluated by microscopic observation.

Antibodies. Rabbit polyclonal anti-*Tc*HTE antibodies were obtained using the p1*Tc*HTE peptide expressed as a TRX.HIS-fusion protein, as it was described in the Supporting Information S1. All experiments were approved by the Institutional Committee of Animal Care and Use of the Facultad de Ciencias Bioquímicas y Farmacéuticas (School of Biochemical and Pharmaceutical Science), Universidad Nacional de Rosario, Argentina, and conducted according to specifications of the US National Institutes of Health guidelines for the care and use of laboratory animals (file number 935/2015).

Effect of heme on epimastigote growth and *Tc*HTE protein accumulation.

Epimastigotes (WT) grown in LIT-10% FBS with 5 µM hemin for 48 h were collected, washed with PBS and challenged to grow in LIT-10% FBS without (0 µM) or supplemented with 5, 20 or 50 µM hemin. The number of cells was monitored daily for 14 days. One dilution to the initial condition was made on day 7. On the third- and seventh-days samples were collected by centrifugation at 2000 *g* for 5 minutes, washed twice with PBS and prepared for optic microscopy as described below. Also, aliquots were lysed (1 x 10^6 parasites/µl) with lysis buffer (8 M Urea, 30 mM HEPES, pH 8) for Western Blot assays.

Effect of heme on *Tc*HTE protein accumulation in amastigotes

To obtain the intracellular amastigotes, Vero cells were cultured as described above. After 24 h of incubation in DMEM-2% FBS, cells were incubated with trypomastigotes WT in a ratio of 10 trypomastigotes/cell (MOI=10, multiplicity of infection) for 4 h to let the infection progress. After that, the cells were washed twice with PBS and 2 ml of DMEM-2% FBS was added. 24 h post-infection, hemin was added at a final concentration of 20 µM. After 24 h of incubation (with or without extra hemin), intracellular amastigotes were purified by cell disruption and protein extracts were obtained for Western blot assay by lysing the cells with lysis buffer as previously described (29).

Effect of *Tc*HTE over-expression on amastigote proliferation.

To analyze amastigote proliferation, the Vero cell line was plated on 24 well plates with coverslips in DMEM-2% FBS. After 24 h, cells were incubated 4 h with Cell-derived trypomastigotes, WT or *Tc*HTE-over-expressing ones, at MOI=10. After the infection, the cells were washed twice with PBS and 2 mL of fresh medium were added. 72 h post-infection, infected cells were washed with PBS, and prepared for Giemsa staining and microscopic analysis as described below. Amastigotes from 183 infected cells for each group were counted by direct observation under microscope.

Western blot.

Total protein from cell-free extracts obtained from epimastigotes, trypomastigotes and amastigotes were prepared as described previously (29). Samples were heated at 42 °C for 30 minutes in loading buffer (1.8% SDS, 5% glycerol and 0.5% β-mercaptoethanol), 5 x 10^6 cells/well were resolved by electrophoresis on a 15% SDS polyacrylamide gel and electrotransferred onto nitrocellulose membranes (Amersham). The membranes were blocked in 5% non-fat dry milk in PBS-T (PBS plus 0.1% Tween 20) over night at 4 °C. *Tc*HTE detection was performed with rabbit anti-*Tc*HTE antibodies (1:5000). Bound antibodies were detected with peroxidase-labeled anti-rabbit IgG (1:30000) (Calbiochem), and ECL Prime Western Blotting Detection kit (GE Healthcare). The membranes were stripped 30 minutes at 50 °C with Stripping Buffer (2% SDS, 100 mM β-mercaptoethanol, 62.5 mM Tris pH 8, blocked and

blotted against α-tubulin clone TAT-1 antibodies (a gift from K. Gull, University of Oxford, U.K.) as a loading control.

mRNA isolation, reverse transcription PCR (RT-PCR) and quantitative real-time PCR (qRT-PCR). The following samples were used to obtain mRNA from different life-cycle stages of *T. cruzi*: epimastigotes cultured in LIT-10% FBS supplemented with or without 20 µM hemin for 3 days were collected, washed with PBS and cultured in LIT-10% FBS supplemented with 0, 5 or 20 µM hemin for 18 h. Also, trypomastigotes, amastigotes and epimastigotes maintained in LIT-10% FBS supplemented with 5 µM hemin were used for mRNA purification as we previously described with minor modifications (30). Briefly, the total mRNA was obtained using TRI Reagent® (Molecular Research Center, Inc., # TR 118). The RNA preparations were treated with RNase-free DNase I (Fermentas, Life Sciences) and their quality and concentration were checked following standard procedures (31). Each RNA extraction was carried out by triplicate. cDNAs of *T. cruzi* were synthesized through a RT reaction (M-MuLV, Thermo-Scientific) using 0.5 µg of total RNA. mRNA analysis by quantitative Real-time PCR was performed in an Applied Biosystems StepOne™ Real-Time PCR System Thermal Cycling Block using the SYBRgreen fluorescence quantification system (Fermentas). The standard PCR conditions were: 95 °C (10 min), and then 40 cycles of 94 °C (1 min), 60 °C (1 min) and 72 °C (2 min), followed by the denaturation curve. The primer designs were based on nucleotide sequences of *T. cruzi* CL Brenner Esmeraldo-like genes coding for *Tc*HTE and glyceraldehyde-3-phosphate dehydrogenase (GAPDH) (TriTrypDB accession numbers for *Tc*HTE: TcCLB.511071.190 and GAPDH: TcCLB.506943.50). The sequences of the primers used are listed below. The data were analyzed using StepOne™ software v 2.1. The fold-change in the expression of the transcripts was obtained using the comparative method ($\Delta\Delta C_t$) (32). The epimastigote stage at 5 µM hemin was used as the reference condition for both genes. Primers for qRT-PCR: *Tc*HTEss 5´-TAATTATTGGGCGGCGGCT-3´, *Tc*HTEas 5´-GAAGTACGAACTCCCCGTCC-3´ (product 235 bp); and GAPDHss 5´-GTGGCAGCACCGGTAACG-3´, GAPDHas 5´-CAGGTCTTTCTTTTGCGAATAGG-3´ (product 110 bp). The differences in the transcriptional level among the different stages were compared using One-way Anova, followed by Bonferroni's multiple comparison test. For this purpose, the software GRAPHPAD PRISM version 5.00 for Windows (GraphPad Software, San Diego, CA) was used. The significance level (P value) was determined with a confidence interval of 95% in a two-tailed distribution.

Optic microscopy

Epimastigotes were fixed with formaldehyde 3.7% (w/v) in PBS, washed twice with PBS and settled on poly-L-lysine-coated microscope slides. Parasites were stained with Giemsa reagent for 20-30 minutes, washed with stabilized water and mounted for microscopic analysis. Infected cells bearing *T. cruzi* amastigotes grown over these coverslips were washed with PBS and fixed with pure methanol for 3 minutes. Then, the cells were washed again, stained with Giemsa reagent and mounted with Canada balsam on microscope slides for microscopic analysis

Confocal microscopy

The following samples were prepared for confocal microscopy analysis: epimastigotes incubated with the HAs (15 µM HAs and 5 µM hemin) for three days as it is described below to monitor HAs incorporation, recombinant trypomastigotes obtained from the supernatant of infected cells and the infected cells containing recombinant amastigotes to track r*Tc*HTE.HIS-GFP localization. Epimastigotes and trypomastigotes were collected, washed with PBS and fixed with formaldehyde 3.7% (w/v) in PBS. After that, they were washed twice with PBS, suspended in 40 µl of PBS, settled on poly-L-lysine-coated microscope slides and mounted with VectaShield reagent. Infected cells with *T. cruzi* amastigotes grown over coverslips were washed with PBS and fixed with pure methanol for 3 minutes. Then, the cells were washed again and also mounted with VectaShield reagent for microscopic analysis.

All the images were acquired with confocal microscopes Nikon Eclipse TE-2000-E2 or Zeiss LSM880 and were processed using the ImageJ software (33). The emission of the samples treated with HAs displaying red fluorescence was registered at 605/75 nm. The emission of the samples containing GFP fusion proteins was registered at 515/30 nm. The emission of the

samples treated with DAPI was registered at 450/30 nm.

Epimastigote growth curve with HAs

Epimastigotes grown in LIT-10% FBS with 5 µM hemin for 48 h were collected, washed with PBS and challenged to growth in LIT-10% FBS supplemented with 5 and 20 µM hemin, or 5 µM hemin plus 15 µM heme analogs (ZnMP and SnMP). Parasites were maintained in mid-log phase by successive dilution every 2 days and growth was monitored for 9 days. On the third day samples were collected and prepared for confocal analysis as described above or to measure direct fluorescence as described below.

Heme content analysis

The heme content was quantified by the alkaline pyridine method described in Berry et al. (34) as we described previously (29) with minor modifications. Briefly, 150 x 10^6 *T. cruzi* epimastigotes were collected and washed twice with PBS. Samples were suspended in 500 µL of PBS and then combined with 500 µl of a solution containing 0.2 N NaOH and 40% (v/v) pyridine. The oxidized and reduced (by addition of sodium dithionite) spectra were recorded between 450 nm and 700 nm. The 557 nm peak identified in the differential -reduced minus oxidized- spectrum was used to estimate the heme concentration (ε^{557} = 23.98 mM^{-1} cm^{-1} (34)).

Fluorescence Intensity analysis

Twenty million epimastigote cells treated with HAs (obtained from the growth curve) were suspended with 500 µL of lysis buffer (0.5% Triton X-100 in PBS) and disrupted by repeated freezing and thawing cycles. The lysates were centrifuged and the supernatants (total cell extracts) were used to measure fluorescence intensity (FI) in a Varian Eclipse fluorometer: λex = 405 nm, recording the emission spectra between 450 to 650 nm and analyzing the maximal emission at 578 nm for ZnMP, and 574 nm for SnMP. Data are expressed as means ± SD of three independent measurements, normalized by parasite number.

Statistical analysis

The experiments were performed in triplicate, and the data is presented as the mean ± SD (standard deviation) except when is informed. All the assays were independently reproduced at least 2–4 times. Statistically significant differences between groups were assessed using One way ANOVA followed by Dunnet multiple comparison test (intracellular heme), Mann-Whitney test (amastigote proliferation) or One way ANOVA followed by Bonferroni´s multiple comparison test (mRNA analysis), as appropriate (GRAPHPAD PRISM version 5.00 for Windows, GraphPad Software, San Diego, CA).

Acknowledgments: We are grateful to Rodrigo Vena for his help in the acquisition of confocal microscopy images, and also to Dolores Campos for the assistance in cell culture procedures.

Conflict of interest: The authors declare that they have no conflict of interest with the content of this article.

References

1. Ponka, P. (1999) Cell biology of heme. *Am. J. Med. Sci.* **318**, 241–256
2. Yin, L., Wu, N., and Lazar, M. A. (2010) Nuclear Receptor Rev-Erbα: A Heme Receptor that Coordinates Circadian Rhythm and Metabolism. *Nucl. Recept. Signal.* **8**, nrs.08001
3. Tsiftsoglou, A. S., Tsamadou, A. I., and Papadopoulou, L. C. (2006) Heme as key regulator of major mammalian cellular functions: Molecular, cellular, and pharmacological aspects. *Pharmacol. Ther.* **111**, 327–345
4. Faller, M., Matsunaga, M., Yin, S., Loo, J. A., and Guo, F. (2006) Heme is involved in microRNA processing. *Nat. Struct. Mol. Biol.* **14**, 23–29
5. Hamza, I., and Dailey, H. a. (2012) One ring to rule them all: Trafficking of heme and heme synthesis intermediates in the metazoans. *Biochim. Biophys. Acta - Mol. Cell Res.* **1823**, 1617–1632
6. Choby, J. E., and Skaar, E. P. (2016) Heme Synthesis and Acquisition in Bacterial Pathogens. *J. Mol. Biol.* 10.1016/j.jmb.2016.03.018
7. Panek, H., and O'Brian, M. R. (2002) A whole genome view of prokaryotic haem biosynthesis. *Microbiology*. **148**, 2273–2282
8. Kořený, L., Oborník, M., and Lukeš, J. (2013) Make It, Take It, or Leave It: Heme Metabolism of Parasites. *PLoS Pathog.* 10.1371/journal.ppat.1003088
9. Tripodi, K. E. J., Menendez Bravo, S. M., and Cricco, J. A. (2011) Role of heme and heme-proteins in trypanosomatid essential metabolic pathways. *Enzyme Res.* **2011**, 873230
10. Tyler, K. M., and Engman, D. M. (2001) The life cycle of Trypanosoma cruzi revisited. *Int. J. Parasitol.* **31**, 472–481
11. Rajagopal, A., Rao, A. U., Amigo, J., Tian, M., Upadhyay, S. K., Hall, C., Uhm, S., Mathew, M. K., Fleming, M. D., Paw, B. H., Krause, M., and Hamza, I. (2008) Haem homeostasis is regulated by the conserved and concerted functions of HRG-1 proteins. *Nature*. **453**, 1127–1131
12. Huynh, C., Yuan, X., Miguel, D. C., Renberg, R. L., Protchenko, O., Philpott, C. C., Hamza, I., and Andrews, N. W. (2012) Heme uptake by Leishmania amazonensis is mediated by the transmembrane protein LHR1. *PLoS Pathog.* **8**, 36
13. Renberg, R. L., Yuan, X., Samuel, T. K., Miguel, D. C., Hamza, I., Andrews, N. W., and Flannery, A. R. (2015) The Heme Transport Capacity of LHR1 Determines the Extent of Virulence in Leishmania amazonensis. *PLoS Negl. Trop. Dis.* **9**, e0003804
14. Miguel, D. C., Flannery, A. R., Mittra, B., and Andrews, N. W. (2013) Heme uptake mediated by lhr1 is essential for leishmania amazonensis virulence. *Infect. Immun.* **81**, 3620–3626
15. Merli, M. L., Pagura, L., Hernández, J., Barisón, M. J., Pral, M. F., Silber, A. M., and Cricco, J. A. (2016) The Trypanosoma cruzi Protein TcHTE Is Critical for Heme Uptake. *PLoS Negl. Trop. Dis.* 10.1371/journal.pntd.0004359
16. Cabello-Donayre, M., Malagarie-Cazenave, S., Campos-Salinas, J., Gálvez, F. J., Rodríguez-Martínez, A., Pineda-Molina, E., Orrego, L. M., Martínez-García, M., Sánchez-Cañete, M. P., Estévez, A. M., and Pérez-Victoria, J. M. (2016) Trypanosomatid parasites rescue heme from endocytosed hemoglobin through lysosomal HRG transporters. *Mol. Microbiol.* **101**, 895–908
17. Horáková, E., Changmai, P., Vancová, M., Sobotka, R., Abbeele, J. Van Den, Vanhollebeke, B., and Lukeš, J. (2017) The Trypanosoma brucei Tb Hrg protein is a heme transporter involved in the regulation of stage-specific morphological. *J. Biol. Chem.* **292**, 6998–7010
18. Maree, J. P., and Patterson, H.-G. (2014) The epigenome of Trypanosoma brucei: a regulatory interface to an unconventional transcriptional machine. *Biochim Biophys Acta*. **1839**, 743–750
19. Siegel, T. N., Gunasekera, K., Cross, G. A. M., and Ochsenreiter, T. (2011) Gene expression in Trypanosoma brucei: Lessons from high-throughput RNA sequencing. *Trends Parasitol.* **27**, 434–441
20. Lara, F. A., Sant'Anna, C., Lemos, D., Laranja, G. A. T., Coelho, M. G. P., Reis Salles, I., Michel, A., Oliveira, P. L., Cunha-e-Silva, N., Salmon, D., and Paes, M. C. (2007) Heme requirement and intracellular trafficking in Trypanosoma cruzi epimastigotes. *Biochem. Biophys. Res. Commun.* **355**, 16–22

21. Cupello, M. P., Souza, C. F. De, Buchensky, C., Soares, J. B. R. C., Laranja, G. A. T., Coelho, M. G. P., Cricco, J. A., and Paes, M. C. (2011) The heme uptake process in Trypanosoma cruzi epimastigotes is inhibited by heme analogues and by inhibitors of ABC transporters. *Acta Trop.* **120**, 211–218
22. Kořený, L., Lukeš, J., and Oborník, M. (2010) Evolution of the haem synthetic pathway in kinetoplastid flagellates: An essential pathway that is not essential after all? *Int. J. Parasitol.* **40**, 149–156
23. Cabello-Donayre, M., Orrego, L. M., Herráez, E., Vargas, P., Martínez-García, M., Campos-Salinas, J., Pérez-Victoria, I., Vicente, B., Marín, J. J. G., and Pérez-Victoria, J. M. (2019) Leishmania heme uptake involves LmFLVCRb, a novel porphyrin transporter essential for the parasite. *Cell. Mol. Life Sci.* 10.1007/s00018-019-03258-3
24. Cupello, M. P., Souza, C. F., Menna-Barreto, R. F., Nogueira, N. P. A., Laranja, G. A. T., Sabino, K. C. C., Coelho, M. G. P., Oliveira, M. M., and Paes, M. C. (2014) Trypanosomatid essential metabolic pathway: New approaches about heme fate in Trypanosoma cruzi. *Biochem. Biophys. Res. Commun.* **449**, 216–221
25. Lentini, G., Dos Santos Pacheco, N., and Burleigh, B. A. (2018) Targeting host mitochondria: A role for the Trypanosoma cruzi amastigote flagellum. *Cell. Microbiol.* 10.1111/cmi.12807
26. Hanna, D. A., Harvey, R. M., Martinez-Guzman, O., Yuan, X., Chandrasekharan, B., Raju, G., Outten, F. W., Hamza, I., and Reddi, A. R. (2016) Heme dynamics and trafficking factors revealed by genetically encoded fluorescent heme sensors. *Proc. Natl. Acad. Sci.* **113**, 7539–44
27. Yuan, X., Rietzschel, N., Kwon, H., Walter Nuno, A. B., Hanna, D. A., Phillips, J. D., Raven, E. L., Reddi, A. R., and Hamza, I. (2016) Regulation of intracellular heme trafficking revealed by subcellular reporters. *Proc. Natl. Acad. Sci. U. S. A.* **113**, E5144-52
28. Atamna, H., Brahmbhatt, M., Atamna, W., Shanower, G. A., and Dhahbi, J. M. (2015) ApoHRP-based assay to measure intracellular regulatory heme. *Metallomics*. **7**, 309–321
29. Merli, M. L., Cirulli, B. A., Menendez-Bravo, S. M., and Cricco, J. A. (2017) Heme A synthesis and CcO activity are essential for Trypanosoma cruzi infectivity and replication. *Biochem. J.* **474**, 2315–2332
30. Buchensky, C., Almirón, P., Mantilla, B. S., Silber, A. M., and Cricco, J. A. (2010) The Trypanosoma cruzi proteins TcCox10 and TcCox15 catalyze the formation of heme A in the yeast Saccharomyces cerevisiae. *FEMS Microbiol. Lett.* **312**, 133–141
31. Sambrook, J., and Russell, D. W. (2001) *Molecular Cloning: A Laboratory Manual*, Molecular Cloning: A Laboratory Manual, Cold Spring Harbor Laboratory Press
32. Bookout, A. L., Cummins, C. L., Mangelsdorf, D. J., Pesola, J. M., and Kramer, M. F. (2006) High-throughput real-time quantitative reverse transcription PCR. *Curr. Protoc. Mol. Biol.* **Chapter 15**, Unit 15.8
33. Schindelin, J., Arganda-Carreras, I., Frise, E., Kaynig, V., Longair, M., Pietzsch, T., Preibisch, S., Rueden, C., Saalfeld, S., Schmid, B., Tinevez, J.-Y., White, D. J., Hartenstein, V., Eliceiri, K., Tomancak, P., and Cardona, A. (2012) Fiji: an open-source platform for biological-image analysis. *Nat Meth*. **9**, 676–682
34. Berry, E. a, and Trumpower, B. L. (1987) Simultaneous determination of hemes a, b, and c from pyridine hemochrome spectra. *Anal. Biochem.* **161**, 1–15

FOOTNOTES

The research leading to these results has, in part, received funding from UK Research and Innovation via the Global Challenges Research Fund under grant agreement 'A Global Network for Neglected Tropical Diseases' grant number MR/P027989/1, and ANPCyT (National Agency of Scientific and Technological Promotion) grant no. PICT 2015-2437 to J.A.C.
JAC is a researcher of CONICET (National Research Council of Science and Technology), LP and MLM had a fellowship from CONICET to conduct their Ph.D., ET has a fellowship of ANPCyT associated to grant no. PICT 2015-2437.

The abbreviations used are: *Tc*HTE, *T. cruzi* Heme Transport Enhancer; r*Tc*HTE.His-GFP, recombinant *Tc*HTE; HRG, Heme-response Gene; LHR1, *Leishmania* heme response 1; *Tb*HRG, *T. brucei* heme-responsive gene; TMD, transmembrane domain; qRT-PCR, quantitative real-time PCR; SnMP, Sn(IV) mesoporphyrin; ZnMP, Zn(II) mesoporphyrin; LIT, Liver Infusion Tryptose; DMEM, Dulbecco's modified Eagle's medium; FBS, fetal bovine serum; DAPI, 4',6-Diamidino-2-Phenylindole; GFP, green fluorescent protein; MOI, multiplicity of Infection; WT, wild-type.

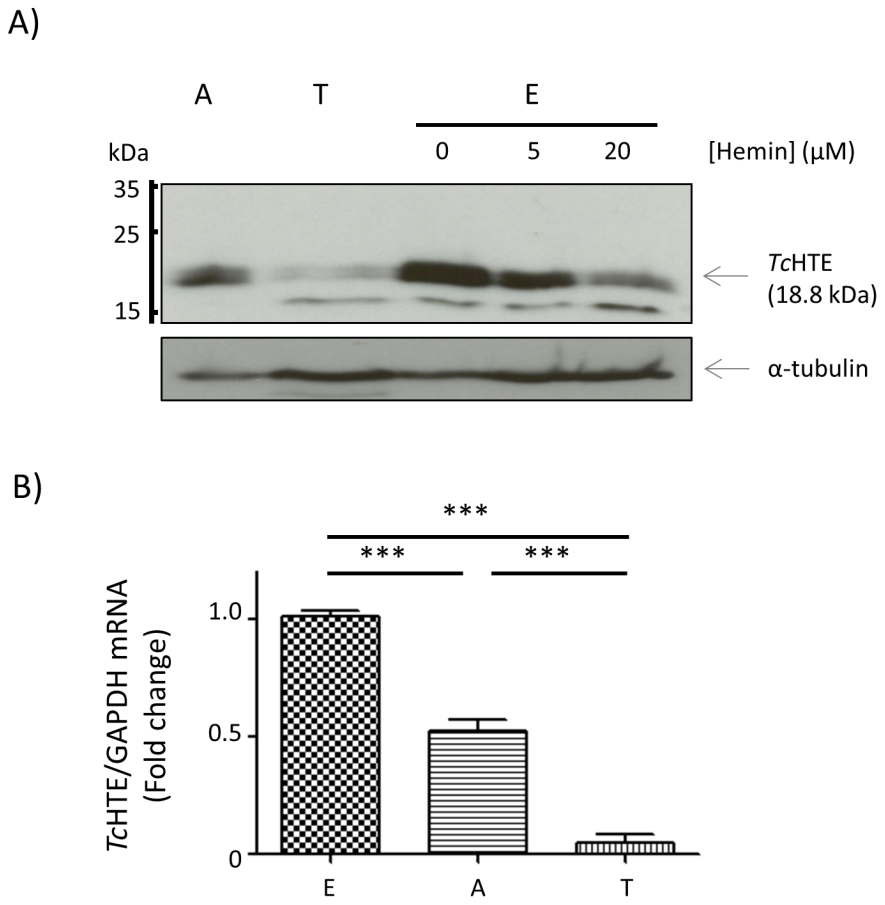

Figure 1: Comparative expression of *Tc*HTE in different developmental stages.
A. Endogenous expression of *Tc*HTE in different life-cycle stage of *T. cruzi*. Western Blot analysis using anti-*Tc*HTE antibodies shows the accumulation of *Tc*HTE protein, being it higher in replicative stages (amastigotes and epimastigotes). Also, the accumulation of *Tc*HTE in epimastigotes changes according to heme concentration available in the medium after 3 days of incubation (LIT-10% FBS supplemented without or with 5 and 20 μM hemin). α-tubulin was used as a loading control. B. *Tc*HTE transcript level at different developmental stages. qRT-PCR of the *Tc*HTE transcript in epimastigotes from axenic culture (E), intracellular amastigotes (A) and trypomastigotes (T) of *T. cruzi*. Transcripts from intracellular amastigotes and cells derived trypomastigotes were compared with epimastigotes grown in LIT-10% FBS plus 5 μM hemin, which was set to 1. GAPDH was used for normalization. Statistical significance was determined by One-way ANOVA followed by Bonferroni´s multiple comparison test. $p<0.0001$.

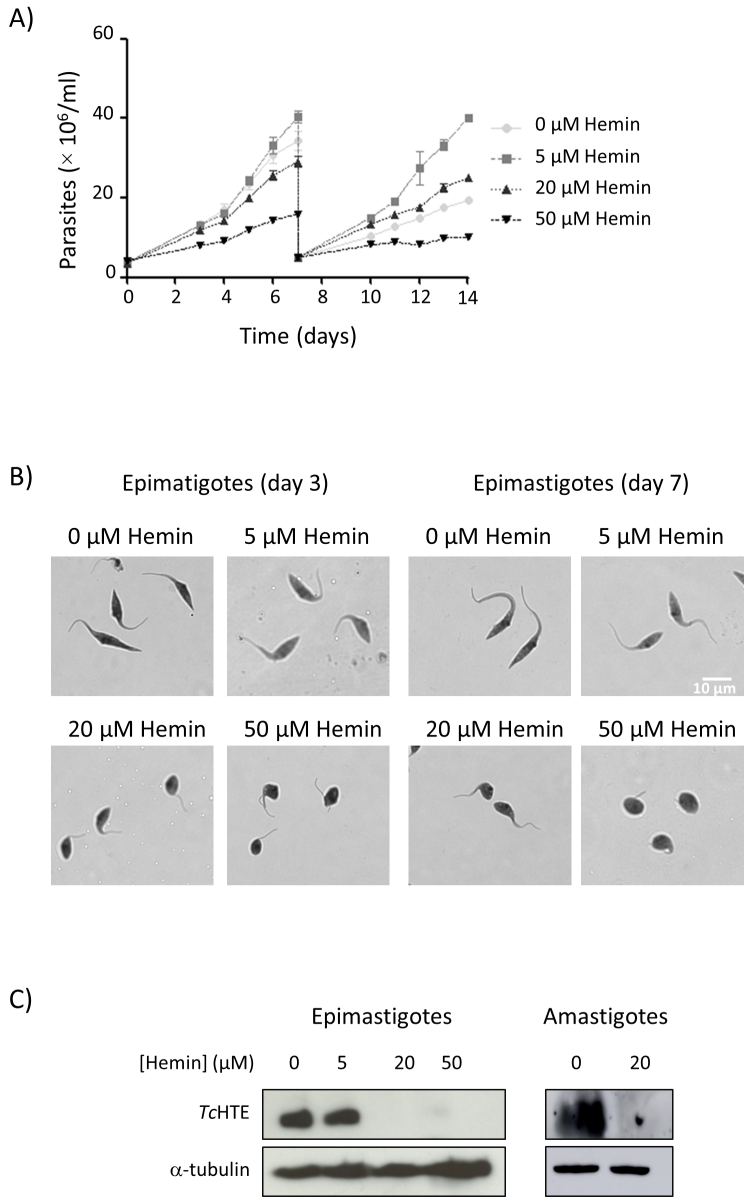

Figure 2: Changes in heme concentration in the medium affects epimastigote proliferation and *Tc*HTE expression.
A. Growth curves of epimastigotes in LIT-10% FBS plus 0, 5, 20 and 50 µM hemin, monitored for 14 days, with a dilution to the initial concentration in fresh medium at day 7. Previously, parasites were maintained 72 h in LIT-10% FBS without hemin. Data is presented as mean ± SD of three independent assays. B. Giemsa staining of epimastigotes cultured in LIT-10% FBS with 0, 5, 20 or 50 µM hemin for 3 and 7 days. C. Endogenous expression of *Tc*HTE in epimastigotes and amastigotes incubated with different amounts of hemin added to the medium. Western Blot analysis using anti-*Tc*HTE antibodies shows a clear signal corresponding to *Tc*HTE protein in epimastigotes and amastigotes incubated without or with low hemin after 72 h of incubation. The signal of *Tc*HTE almost disappears when hemin is added at higher quantities. α-tubulin was used as a loading control.

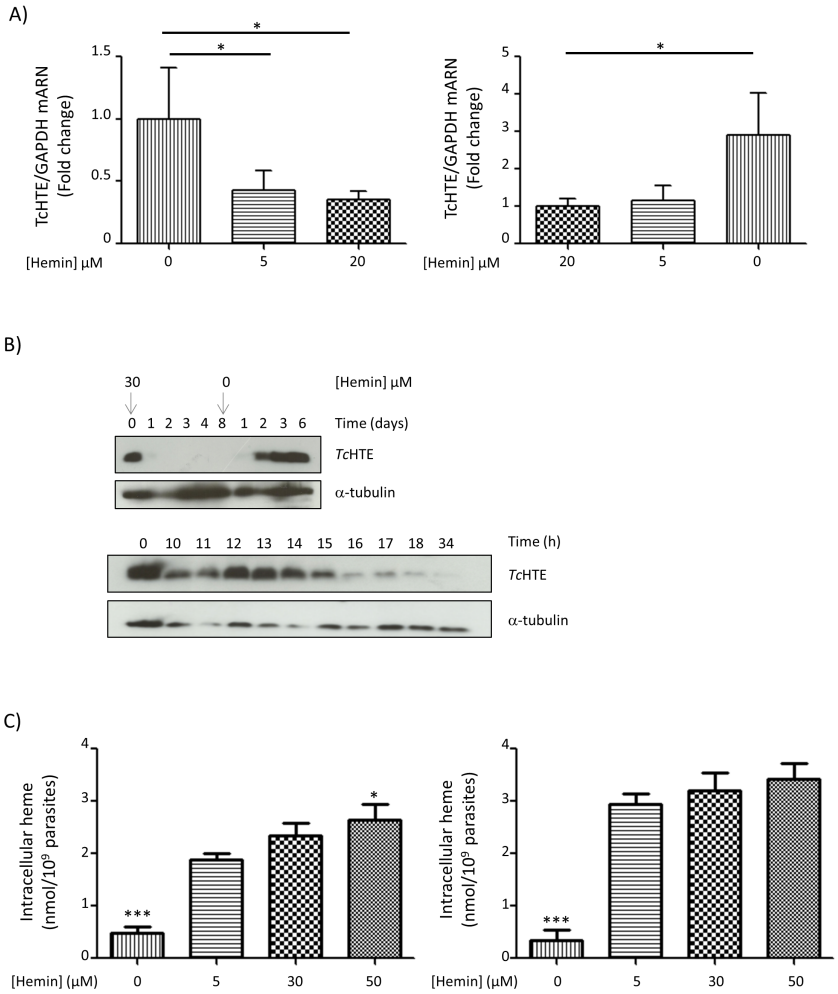

Figure 3: *Tc*HTE expression responds to heme at mRNA and Protein level.
A. Quantitative RT-PCR of *T. cruzi* epimastigotes undergo changes in hemin concentration in the medium. Epimastigotes were cultured in LIT-10% FBS without (left panel) or with 20 µM hemin (right panel). Three days after, cells were collected, washed with PBS and cultured in LIT-10% FBS supplemented with 0, 5 or 20 µM heme for 18 h and *Tc*HTE mRNA was quantified by qRT-PCR. *Tc*HTE values were normalized respect to GAPDH. Statistical significance was determined by One-way ANOVA followed by Bonferroni's multiple comparison test. $p<0.05$. B: *Tc*HTE protein responds to heme availability. Western blot assay, using anti-*Tc*HTE antibodies to recognize endogenous protein in total extracts of epimastigotes. Upper panel: Parasites were growth in LIT medium supplemented with 5 µM hemin and then incubated with 30 µM hemin (day 0). Samples were taken every day for a week. The remaining epimastigotes were washed and maintained in LIT-10% FBS without hemin (day 8) and samples were taken every day for another week. Bottom panel: Parasites were grown in LIT-10% FBS supplemented with 5 µM hemin and then incubated with 30 µM hemin. Samples were taken every hour. Anti α-tubulin was used as loading control. C. Intracellular heme content determined by pyridine method of Dm28c epimastigotes grown in LIT-10% FBS plus 0, 5, 30 and 50 µM hemin, for 18 h (left panel) and 24 h (right panel). Data is presented as mean ± SD of three independent assays. Statistical significance was determined by One-way ANOVA followed by Dunnet multiple comparison test. 5 µM hemin was chosen as control. *$p < 0.1$, ***$p < 0.01$.

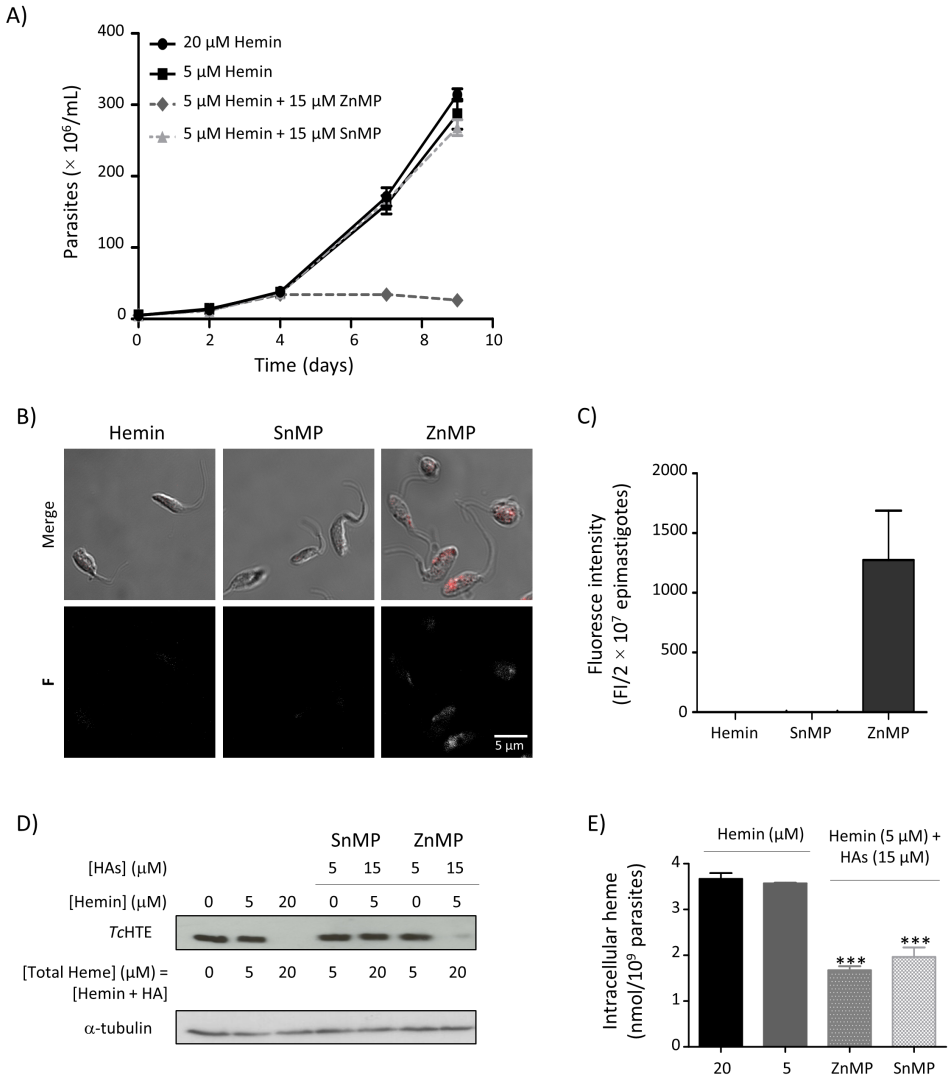

Figure 4: Heme analogs affect epimastigote growth and *Tc*HTE accumulation.
A. Growth curves of *T. cruzi* epimastigotes in LIT-10% FBS plus 5, 20 µM hemin or 5 µM hemin plus 15 µM of HAs (ZnMP and SnMP), monitored for 9 days. Parasites were maintained in exponential growth by periodic dilution every two days in fresh medium. Previously, parasites were maintained 72 h in LIT-10% FBS without hemin. Data is presented as mean ± SD of three independent assays. B: Confocal microscopy of epimastigotes incubated with 5 µM hemin or 5 µM hemin plus 15 µM of the different HAs for 3 days. C: Fluorescence intensity. Fluorescence intensity (FI) from cell-free extracts were obtained after 3 days of incubation of epimastigotes with 5 µM hemin or 5 µM hemin plus 15 µM of the different HAs. The experimental data is presented as the mean ± SD of three independent replicates. D: Western blot assay, using anti-*Tc*HTE antibodies to recognize endogenous protein in total extracts of epimastigotes cultured with 0, 5 or 20 µM hemin, 5 µM HAs or 5 µM hemin plus 15 µM HAs for four days. Anti α-tubulin was used as a loading control. E: Intracellular heme content determined by pyridine method of DM28c epimastigotes grown in LIT-10% FBS plus 5, 20 µM hemin or 5 µM hemin plus 15 µM HAs, for 72 h. Data is presented as mean ± SD of three independent assays. Statistical significance was determined by One-way ANOVA followed by Dunnet multiple comparison test, 5 µM hemin was chosen as control. ***$p < 0.01$.

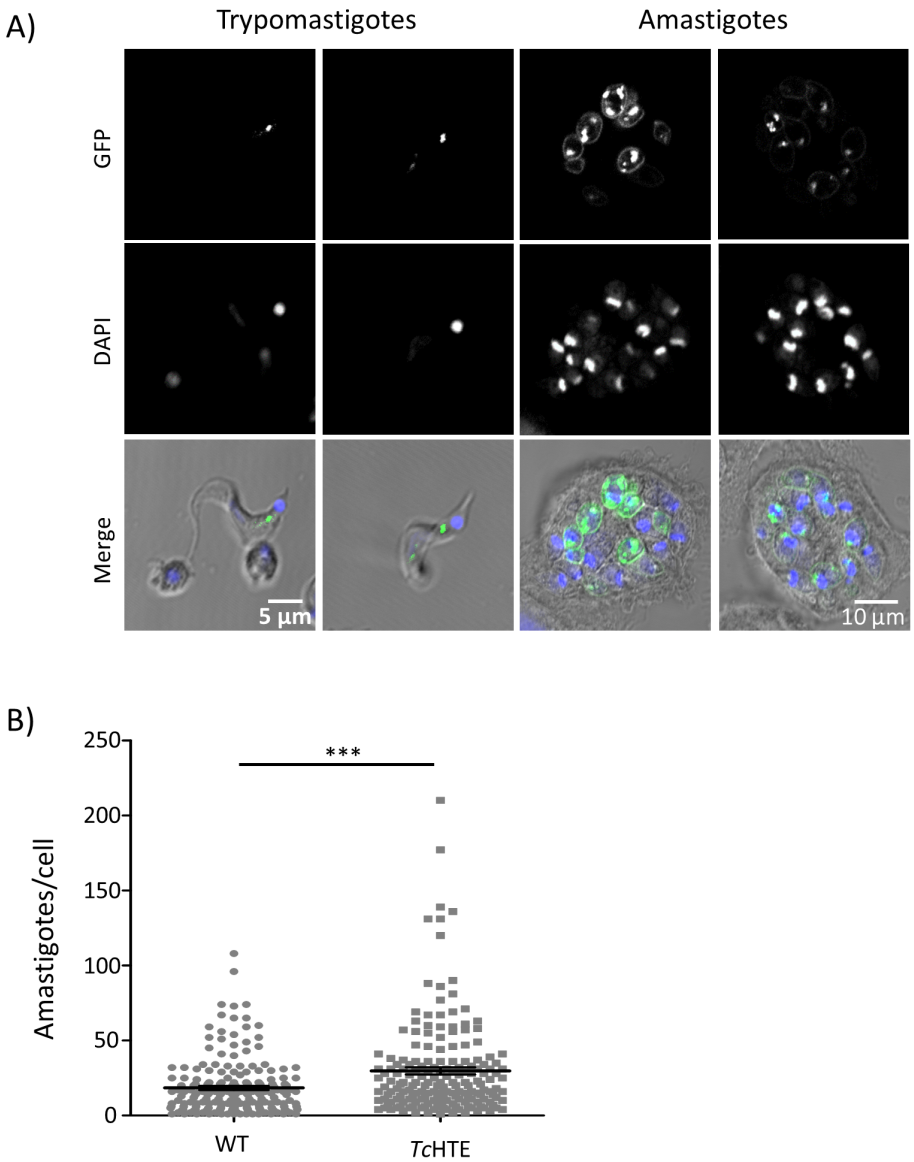

Figure 5: Over-expression of r*Tc*HTE.His-GFP in *T. cruzi*.
A. Cellular localization of r*Tc*HTE.HIS-GFP in trypomastigotes and intracellular amastigotes. Confocal microscopy images of trypomastigotes and amastigotes expressing r*Tc*HTE.HIS-GFP. r*Tc*HTE.HIS-GFP green, DAPI blue. B: Over-expression of *Tc*HTE stimulates amastigotes proliferation. Vero cells were infected with wild type parasites or parasites that over-express r*Tc*HTE.HIS-GFP. 72 h after infection, cells were fixed and stained with Giemsa reagent. Intracellular amastigotes were counted from more than 180 cells for each condition. Statistical significance was determined by Mann-Whitney test. The experimental data is presented as the mean ± SEM. ***$p < 0.0001$.

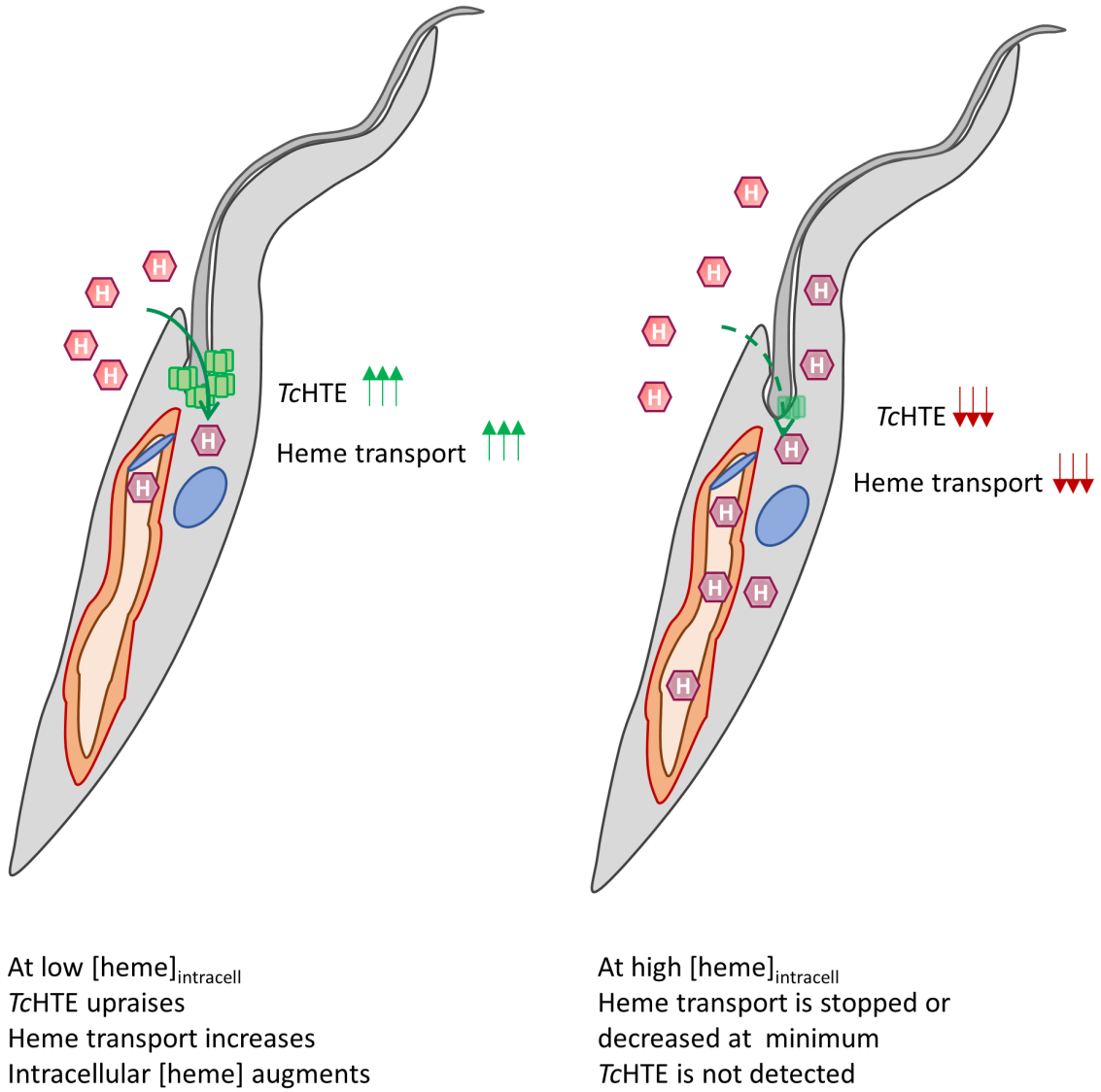

Figure 6: Scheme representing a proposed model for *Tc*HTE/*Tc*HRG function in heme transport. When epimastigotes senses low intracellular heme, augment *Tc*HTE synthesis and assembly in the flagellar pocket and heme uptake increases. Once intracellular heme raises the optimal quota or exceeds it, *Tc*HTE is downregulated and heme import is maintained low, keeping the heme flux at stationary level.

SUPPORTING INFORMATION

Trypanosoma cruzi senses intracellular heme levels and regulates heme homeostasis by modulating *Tc*HTE protein expression

Lucas Pagura*[†1], Evelyn Tevere*, Marcelo L. Merli*[2], Julia A. Cricco*[†3]

From the *Instituto de Biología Molecular y Celular de Rosario (IBR), Consejo Nacional de Investigaciones Científicas y Técnicas CONICET – Facultad de Ciencias Bioquímicas y Farmacéuticas, Universidad Nacional de Rosario UNR. Suipacha 531, S2002LRK, Rosario, Argentina.

[†]Área Biofísica, Departamento de Química Biológica, Facultad de Ciencias Bioquímicas y Farmacéuticas, Universidad Nacional de Rosario UNR. Suipacha 531, S2002LRK, Rosario, Argentina.

Supporting Information S1. Polyclonal antibodies against *Tc*HTE (anti-*Tc*HTE)

Analysis of the *Tc*HTE protein sequence. A bioinformatic analysis of *Tc*HTE protein sequence was carried out to select suitable regions to target for polyclonal antibodies. The prediction of transmembrane topology and antigenic regions were performed using the free access software from EXPASY Proteomics Service site (http://ca.expasy.org). To predict transmembrane topology, TMHMM Server v2.0 (http://www.cbs.dtu.dk/services/ TMHMM/) (1, 2) as well as TMPRED software were used (3). Preditop software (4) was used to predict antigenic regions. A predicted high-antigenic C- terminal region of the protein (p1*Tc*HTE, from aminoacid 120 to 171) was selected as a target for polyclonal antibodies production.

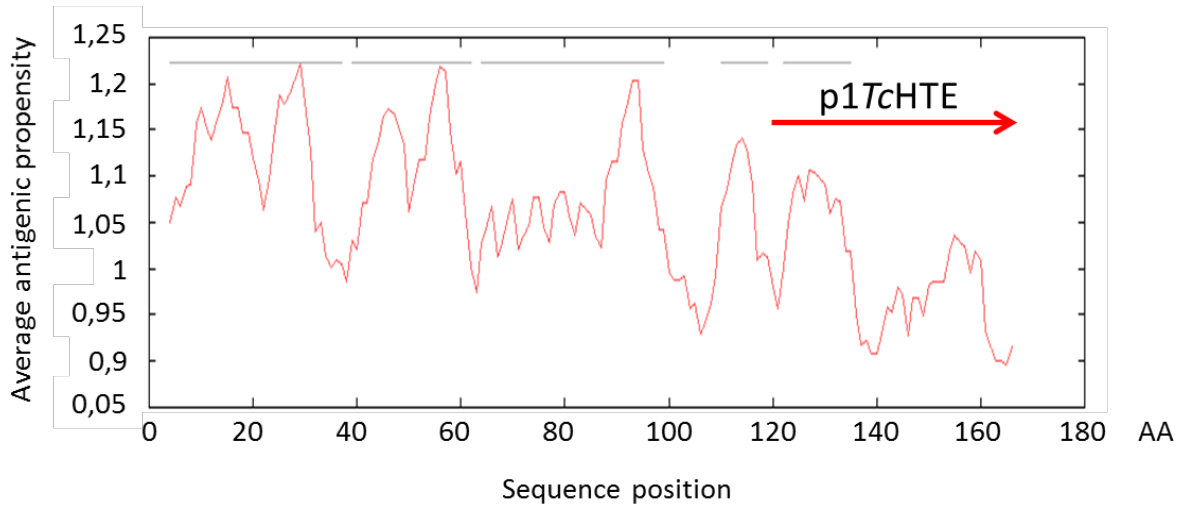

Supporting Figure S1. Bioinformatic prediction of antigenic regions of *Tc*HTE protein. Analysis of antigenic regions performed with Preditop. Fragment p1*Tc*HTE is shown with a red arrow.

DNA manipulations. The *T. cruzi* codifying sequence of *Tc*HTE was previously obtained in the laboratory (5). The primers designed to amplify the DNA fragment *p1TcHTE* are listed in Supporting Table S1, they introduce the restriction sites *Bam*HI and *Xho*I at the 5'- and 3´-end, respectively. The PCR steps were: 2 min at 94 °C; then 30 cycles of 25 s at 94 °C, 30 s at 58 °C and 40 s at 72 °C; and finally, 10 min at 72 °C. PCR products were purified and cloned into pET-32a vector (Novagen®) producing the p*TRX.HIS-p1TcHTE* plasmid, in order to express antigenic fragments as TRX.HIS-fusion protein (TRX.HIS-p1*Tc*HTE). Isolation of plasmidic DNA and PCR products, digestions with restriction enzymes, ligation reactions and agarose gel electrophoresis were carried out by conventional methods (6).

Fragment	**Primer**	**5´-3´ sequence**
p1TcHTE (195pb)	FP_*p1TcHTE*	TCCGGATCCATGATGGCCGCAAAGTGGTG *Bam*HI
	RP_*TcHTE*	CCGCTCGAGTTAATGATGATGATGATGATGACC-CATAATATCTGCGTTCTTTTCG *Xho*I

Supporting Table S1. Primers used to amplify fragment *p1TcHTE*

Protein purification. *E. coli* BL21(DE3)pLysS cells transformed with p*TRX.HIS-p1TcHTE* were used to over-express and purify the fusion protein TRX.HIS-p1*Tc*HTE. The expression of *TRX.HIS-p1TcHTE* was induced by the addition of 0.15 mM IPTG, overnight at 24 °C. Then, cells were collected, suspended with lysis buffer (50 mM Tris:HCl pH 8, 1 mM PMSF, 5 mM $MgCl_2$, 0.1 µg/ml DNase) and disrupted by sonication. After that, the lysate was clarified by centrifugation at 15000 × *g* and 4 °C for 20 min and TRX.HIS-p1*Tc*HTE protein was recovered from the supernatant by affinity chromatography (batch protocol) using Ni-NTA agarose (QIA expressionist) following the manufacturer specifications.

Polyclonal antibodies against *Tc*HTE (anti-*Tc*HTE). The purified TRX.HIS-p1*Tc*HTE was used to obtain antiserum from rabbit containing polyclonal antibodies against *Tc*HTE as we previously reported (7) following described procedures (8, 9).

***Tc*HTE recognition by polyclonal anti-*Tc*HTE antibodies contained in the immune serum.** We tested if the immune serum containing polyclonal anti-*Tc*HTE antibodies selectively recognize *Tc*HTE in epimastigotes by Western blot assay as it is shown in Supporting Figure S2.

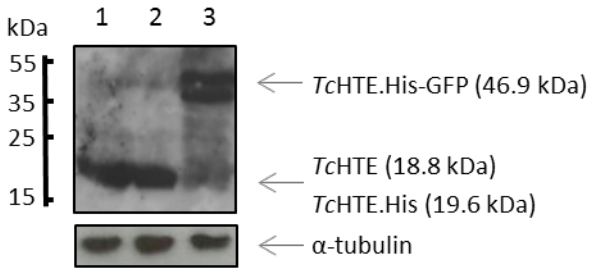

Supporting Figure S2. Western blot assay against total extracts of (lane 1) epimastigotes Dm28c WT, (lane 2) epimastigotes Dm28c overexpressing the recombinant protein *Tc*HTE.His (lane 3) epimastigotes Dm28c overexpressing the recombinant protein *Tc*HTE.His-GFP, probed with anti-*Tc*HTE immune serum (1/5000). Parasites were previously maintained in LIT-10% FBS

supplemented with 5 µM hemin, and 10 x 10^6 parasites/well were loaded. In lanes 1 and 2 were observed single signals, showing an electrophoretic mobility coincident with the predicted molecular weight (MW) of *Tc*HTE and *Tc*HTE.His (18.8 kDa and 19.6 kDa, respectively), although there is no visible difference between both signals. In lane 3, a double band was detected, presenting an electrophoretic mobility approximated to the expected MW of *Tc*HTE.His-GFP (46.9 kDa). One of these bands could be a degradation product of the recombinant protein as a consequence of the overexpression process or a post-translational modification. Also, a weaker band corresponding to the endogenous *Tc*HTE was visualized. Anti-α-tubulin was used as loading control.

Furthermore, we tested if commercial antibodies anti-6X His tag and anti-GFP recognize the recombinant versions of *Tc*HTE, as shown in Supporting Figure S3.

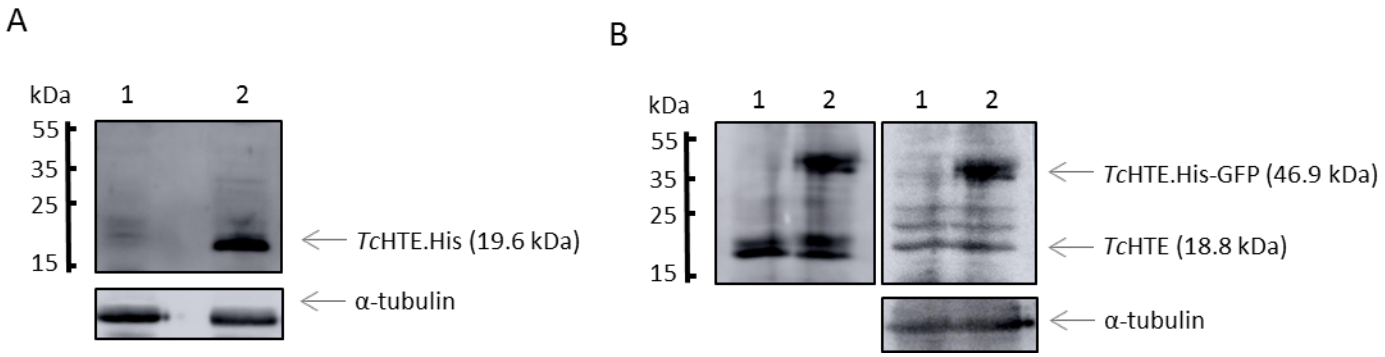

Supporting Figure S3. A) Western blot assay against total extracts of (lane 1) epimastigotes Dm28c WT, (lane 2) epimastigotes Dm28c overexpressing the recombinant protein *Tc*HTE.His. Anti-6X His tag antibodies conjugated to Horseradish Peroxidase (1/5000) (Abcam) detected a unique band corresponding to *Tc*HTE.His in lane 2, whereas the band is absent in lane 1; confirming thus that effectively this recombinant version of *Tc*HTE contains a 6X-His tag. Anti-6X His tag antibodies did not detect *Tc*HTE.His-GFP, since they only recognize N- or C-terminal His tags, and this fusion protein contains the 6X-His tag between *Tc*HTE and GFP.

B) Western blot assay against total extracts of (lane 1) epimastigotes Dm28c WT, (lane 2) epimastigotes Dm28c overexpressing the recombinant protein *Tc*HTE.His-GFP, first incubated

with anti-*Tc*HTE immune serum (1/5000) (left panel), subjected to stripping and then probed with a-GFP antibodies (1/1000) (Santa Cruz Biotechnology) (right panel). When incubated with a-*Tc*HTE antibodies (left panel), the result was similar to Figure S2; but the signal corresponding to endogenous *Tc*HTE in epimastigotes overexpressing *Tc*HTE.His-GFP was more intense. This may be a consequence of the heme starvation. Besides, the signals corresponding to endogenous *Tc*HTE and recombinant *Tc*HTE.His-GFP appeared as double bands. Consistently, in lane 2 of the right panel a signal corresponding to *Tc*HTE.His-GFP was observed. This result confirms the presence of GFP in the recombinant version *Tc*HTE.His-GFP. Also, three weaker signals appeared in both lanes 1 and 2, and they may be unspecific signals.

In both figures (A) and (B), parasites were cultured in LIT-10% FBS without hemin for 48 h, and 10 x 10^6 parasites were loaded in each well. Anti-α-tubulin was used as a loading control.

Supporting Information S2. Phylogenetic analysis of HRG proteins.

Phylogenetic tree. Selected sequences of putative orthologs from kinetoplastids, vertebrates and invertebrates were aligned with ClustalW (10). Transmembrane domain (TMD) predictions were performed with TMHMM Server v. 2.0 (1, 2), presenting the majority of the sequences four TMD. A cladogram was built with the sequences using Phylogeny.fr (11, 12).

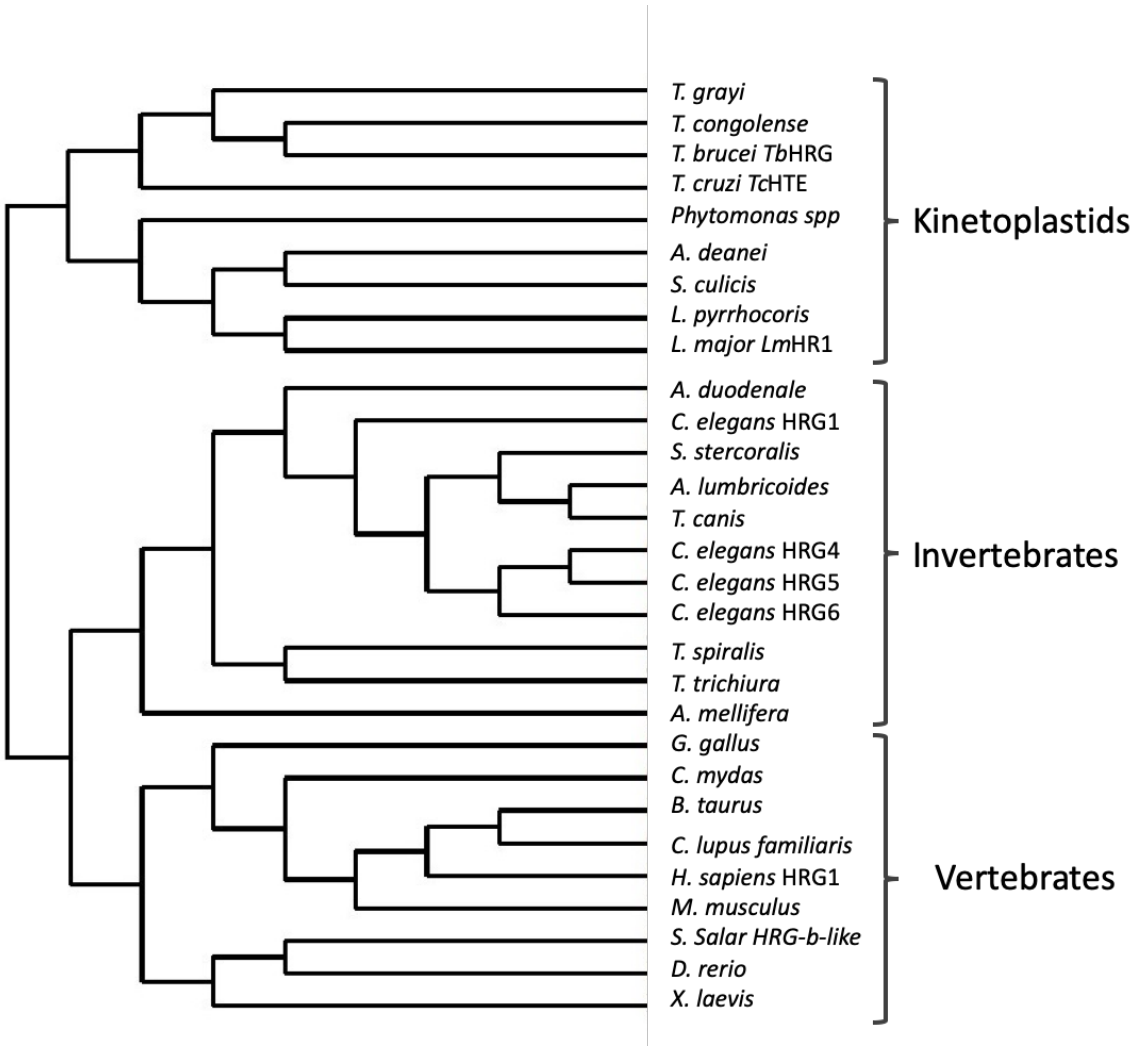

Supporting Figure S4. Cladogram of HRG proteins. Accession numbers: *T. grayi* GenBank Accession Number XP_009310445.1; *T. congolense* UniProt # G0USJ1; *T. brucei Tb*HRG UniProt # Q57YK2; *T. cruzi Tc*HTE UniProt # Q4DHZ7; *Phytomonas spp* UniProt # W6KM41; *A. deanei* UniProt # S9VBR5; *S. culicis* UniProt # S9VQT2; *L. pyrrhocoris* UniProt # A0A0N0DV06; *L. major Lm*HR1 UniProt # Q4QAA7; *A. duodenale* UniProt # A0A0C2G354; *C. elegans* HRG1 UniProt # Q21642; *S. stercoralis* UniProt # A0A0K0EHS5*; A. lumbricoides* UniProt # A0A0M3I5Q9; *T. canis* UniProt # A0A183UJV1; *C. elegans* HRG-4 UniProt # Q20106; *C. elegans* HRG-5 UniProt # Q7YTM8; *C. elegans* HRG-6 UniProt # Q7YTM7; *T. spiralis* UniProt # A0A0V1BW58; *T. trichiura* UniProt # A0A077Z0X3; A*. mellifera* UniProt # A0A088AGX7; G. *gallus* UniProt # Q5ZHU0; *C. mydas* UniProt # M7AQQ6; *B. taurus* UniProt # E1BKJ0; *C. lupus familiaris* UniProt # E2RRB9; *H. sapiens* HRG1 UniProt # Q6P1K1; *M. musculus* UniProt # Q9D8M3; *S. Salar HRG-b-like* UniProt # A0A1S3MGK5;

D. rerio UniProt # Q6ZM28; *X. Laevis* UniProt # A0A1L8HA09. All sequence IDs are UniProt accession numbers, except for *T. grayi* ID (GenBank™ accession number).

References

1. Sonnhammer, E. L., von Heijne, G., and Krogh, a (1998) A hidden Markov model for predicting transmembrane helices in protein sequences. *Proc. Int. Conf. Intell. Syst. Mol. Biol.* **6**, 175–182

2. Krogh, a, Larsson, B., von Heijne, G., and Sonnhammer, E. L. (2001) Predicting transmembrane protein topology with a hidden Markov model: application to complete genomes. *J. Mol. Biol.* **305**, 567–580

3. Hofmann, K., and Stoffel, W. (1993) TMBASE - A database of membrane spanning protein segments. *Biol. Chem. Hoppe. Seyler.* **374**, 166

4. Kolaskar, A. S., and Tongaonkar, P. C. (1990) A semi-empirical method for prediction of antigenic determinants on protein antigens. *FEBS Lett.* **276**, 172–174

5. Merli, M. L., Pagura, L., Hernández, J., Barisón, M. J., Pral, M. F., Silber, A. M., and Cricco, J. A. (2016) The Trypanosoma cruzi Protein TcHTE Is Critical for Heme Uptake. *PLoS Negl. Trop. Dis.* 10.1371/journal.pntd.0004359

6. Sambrook, J., and Russell, D. W. (2001) *Molecular Cloning: A Laboratory Manual*, Molecular Cloning: A Laboratory Manual, Cold Spring Harbor Laboratory Press

7. Merli, M. L., Cirulli, B. A., Menendez-Bravo, S. M., and Cricco, J. A. (2017) Heme A synthesis and CcO activity are essential for Trypanosoma cruzi infectivity and replication. *Biochem. J.* **474**, 2315–2332

8. Clark, A., Befus, D., O'Hashi, P., Hart, F., Schunk, M., Fletch, A., and Griffin, G. (2002) *Guidelines on: antibody production*

9. Hendriksen, C. F. M. (2005) Laboratory Animals and Immunization Procedures: Challenges and Opportunities. *ILAR J.* **46**, 227–229

10. Larkin, M. a., Blackshields, G., Brown, N. P., Chenna, R., Mcgettigan, P. a., McWilliam, H., Valentin, F., Wallace, I. M., Wilm, a., Lopez, R., Thompson, J. D., Gibson, T. J., and Higgins, D. G. (2007) Clustal W and Clustal X version 2.0. *Bioinformatics*. **23**, 2947–2948

11. Dereeper, A., Audic, S., Claverie, J. M., and Blanc, G. (2010) BLAST-EXPLORER helps you building datasets for phylogenetic analysis. *BMC Evol. Biol.* **10**, 8–13

12. Dereeper, A., Guignon, V., Blanc, G., Audic, S., Buffet, S., Chevenet, F., Dufayard, J.-F., Guindon, S., Lefort, V., Lescot, M., Claverie, J.-M., and Gascuel, O. (2008) Phylogeny.fr: robust phylogenetic analysis for the non-specialist. *Nucleic Acids Res.* **36**, W465-9